Catalyst-Free Preparation of Polyhedral Oligomeric Silsesquioxanes Containing Organic–Inorganic Hybrid Mesoporous Nanocomposites

Yuancheng Qin,[1,2] Fanghua Zhu,[2] Meiming Luo,[1] Lin Zhang[2]

[1]*Key Laboratory of Green Chemistry and Technology of Ministry of Education at Sichuan University, College of Chemistry, Sichuan University, Chengdu 610064, People's Republic of China*
[2]*Research Center of Laser Fusion, China Academy of Engineering Physics, Mianyang 621900, China*

Received 15 May 2010; accepted 1 September 2010
DOI 10.1002/app.33353
Published online 16 February 2011 in Wiley Online Library (wileyonlinelibrary.com).

ABSTRACT: A catalyst-free, one-pot method of preparing novel polyhedral oligomeric silsesquioxanes (POSS) containing organic–inorganic hybrid mesoporous nanocomposite at room temperature is reported. Nitrogen sorption analyses gave us a specific surface area of 500.931 m^2/g with a pore volume of 0.563 mL/g and an average pore size of 3.84 nm. The combined results of Fourier transform infrared and solid ^{29}Si-NMR spectroscopy clearly show that the POSS building block was successfully woven into the porous nanostructure without obvious alteration of the characteristics and structure. The material showed good thermal stability. © 2011 Wiley Periodicals, Inc. J Appl Polym Sci 121: 97–101, 2011

Key words: nanocomposites; networks; polycondensation

INTRODUCTION

Highly porous nanoscale structures are critical for a range of emerging technologies because of their increased use in gas storage,[1] gas separation,[2] heterogeneous catalysis,[3] and optics devices.[4,5] Pure inorganic mesoporous materials have their intrinsic limitations, lacking both functionalities and mechanical strength.[6] Inorganic–organic hybrid materials are promising as next-generation functional materials because various functionalities of inorganic and organic species are available, compatible, and cooperative in the design of such materials.[7] Organically functionalized mesoporous silicas have received increasing interest from both scientific and technological viewpoints.[8]

Polyhedral oligomeric silsesquioxanes (POSS) with the formula $R_8Si_8O_{12}$ provide an excellent platform for the synthesis of new inorganic–organic hybrid materials. The octameric form consists of a rigid cubic silica core and a nanopore about 0.3 to 0.4 nm in size.[9] The number and type of the functional corner groups on POSS cages can be readily varied, which makes POSS molecules excellent nanodimensional building blocks for the preparation of various organic–inorganic hybrid nanocomposites.[10–14] Various methods have been developed for preparing POSS-containing organic–inorganic hybrid porous nanocomposites; these include the hydrosilylation of octavinyl–POSS species with octahydrido–POSS species,[9,15,16] self-assembly,[17–19] and hydrolysis.[20] Generally, these synthesis methods need a catalyst and template conditions. Hence, there is a great demand for new strategies suitable for the simple and inexpensive synthesis of porous nanocomposites under mild conditions.

Octa(aminophenyl)silsesquioxane (OAPS) is easily prepared in two steps.[21] As Laine and coworkers[21] reported, OAPS appears to offer excellent potential as a nanoconstruction site for the preparation of materials ranging from high-temperature nanocomposites to precursors for organic light-emitting diodes to multiarmed stars to templates for high-temperature porous materials and so on. Laine and coworkers[22,23] reported OAPS as a model nanobuilding block for rigid, high-temperature hybrid nanocomposite materials. The preparation of OAPS-containing porous materials has not been reported yet. Herein, we report a catalyst-free, one-pot approach in which OAPS reacted with formaldehyde to produce hybrid mesoporous materials under mild conditions.

Correspondence to: L. Zhang (qinyuancheng@sogou.com) or M. Luo (qych19820422@163.com).

Contract grant sponsor: China Academy of Engineering Physics; contract grant number: 2008A0302014.
Contract grant sponsor: National Natural Science Foundation of China; contract grant number: 10976020.
Contract grant sponsor: Program for Changjiang Scholars and Innovative Research Team in University; contract grant number: IRT0846.

EXPERIMENTAL

Materials

Formaldehyde (a 40% water solution), fuming nitric acid [analytic reagent (AR); 95%], Pd/C (5 wt %), triethylamine (AR, 98%), formic acid (an 85% water solution), and $MgSO_4$ (AR, 99%) were purchased from Sinopharm Chemical Reagent Co., Ltd (Shanghai, China), and were used without further purification. Octaphenylsilsesquioxane was purchased from Hybrid Plastics (USA) and was used as received. All other solvents were obtained from commercial sources and were used as received. OAPS was synthesized by the following methods, as described in the literature.[21]

Preparation of OAPS[21]

Octa(nitrophenyl)silsesquioxane (ONPS) (10.0 g, 7.16 mmol) and 5 wt % Pd/C (1.22 g, 0.574 mmol) were charged into a flask with a condenser under N_2. Tetrahydrofuran (THF; 80 mL) and triethylamine (80.0 mL, 0.574 mmol) were then added. The mixture was heated to 60°C, and 85% formic acid (10.4 mL, 0.230 mol) was added slowly at 60°C. After 5 h, the THF layer was separated, and 50 mL of THF and 50 mL of water were added until the slurry formed a black suspension. The suspension and the THF solution separated previously were mixed and filtered through Celite. Another 20 mL of THF and 20 mL of water were added to the flask to dissolve the remaining black slurry, and the suspension was filtered again. All of the filtrates were combined with 50 mL of ethylacetate and washed with H_2O (4×100 mL). The organic layer was dried with 5 g of $MgSO_4$ and precipitated by addition to 2 L of hexane. A white precipitate was collected by filtration, redissolved in 30 : 50 THF/ethyl acetate, and reprecipitated into 1 L of hexane. The obtained powder was dried *in vacuo* (yield = 5.80 g).

Preparation of the hybrid mesoporous materials (P1)

OAPS (0.5505 g, 0.477 mmol) and formaldehyde (0.338 mL, 4.59 mmol) were dissolved in 5 mL of THF. The mixture was stirred at room temperature for 30 min. Then, the precipitate was isolated by filtration over a Büchner funnel and washed with excess acetone, THF, and dichloromethane. The solvent was removed *in vacuo* to afford the materials.

ANAL. Found: C, 41.04%; H, 4.65%; N, 6.89%.

Characterization

Fourier transform infrared (FTIR) spectra of the products in KBr pellets were recorded on a Nicolet 320 FTIR spectrometer (USA). Solid-state ^{29}Si-NMR analyses were conducted on a Infinity plus 300WB spectrometer (USA) operating at 59.62 MHz. The elemental composition was determined with a Carlo Erba 1106 instrument (Italy). Apparent surface areas were determined by the multipoint Brunauer–Emmett–Teller (BET) method from nitrogen adsorption measurements at 77 K with a Quadrasorb SI instrument (USA). Samples were degassed for 6 h before analysis at a temperature of 423 K *in vacuo*. The BET analysis was repeated three times. Adsorption measurements were collected first at a pressure of 10 mbar and then in 30-mbar steps up to 870 mbar. Desorption measurement were then recorded; we started at 850 mbar and then decreased in steps of 50 mbar to 50 mbar, with the final reading recorded at 30 mbar. The pore size distribution was calculated with the cylindrical Barret, Joyner and Halenda (BJH) method,[24] and the BET surface area was calculated from the slope of the isotherm at p/p_0 is relative pressures values up to 0.20. Powder X-ray diffraction (XRD) patterns were obtained at room temperature with a X'Pert PRO instrument (The Netherlands) equipped with a Cu Kα X-ray source (35 kV and 60 mA) with scanning from 2 to 40° 2θ. XRD was repeated three times. Field emission scanning electron microscopy (FESEM) was performed on an FEI Sirion 200 (FEI, The Netherlands). Thermogravimetric analysis (TGA) was performed on a SDT Q600 (TA Instruments-Waters LLC, USA) at a heating rate of 10 K/min under nitrogen. All samples were heated to 1073 K.

RESULTS AND DISCUSSION

Structural analysis

Figure 1(A) shows the FTIR spectra for OAPS and P1. Several distinct peaks were clearly observed. The OAPS spectrum showed a strong υSi—O (cube)[22,23] peak at about 1120 cm^{-1} and primary amine groups at 3590 and 3450 (NH_2 stretching) and 1600 cm^{-1} (NH_2 deformation). Bands that could be attributed to the primary amine group or the carbonyl function of the aldehydes at about 1725 cm^{-1} (C=O stretching) were absent in the spectra of the hybrid materials. Bands that can be attributed to the cage υSi—O at about 1120 cm^{-1} and the second amine group at about 3410 (NH stretching) were found in the spectra of the hybrid materials. The hybrid materials spectra showed a C—H peak at 3000–2800 cm^{-1}. A weak C—N stretching band at about 1295 cm^{-1} was exhibited in the spectra of the hybrid materials.

Characterization of the structures of P1 was accomplished with ^{13}C-NMR and solid-state ^{29}Si-NMR spectroscopy [Fig. 1(B,C)]. The ^{13}C-NMR spectrum of P1 showed signals both for the

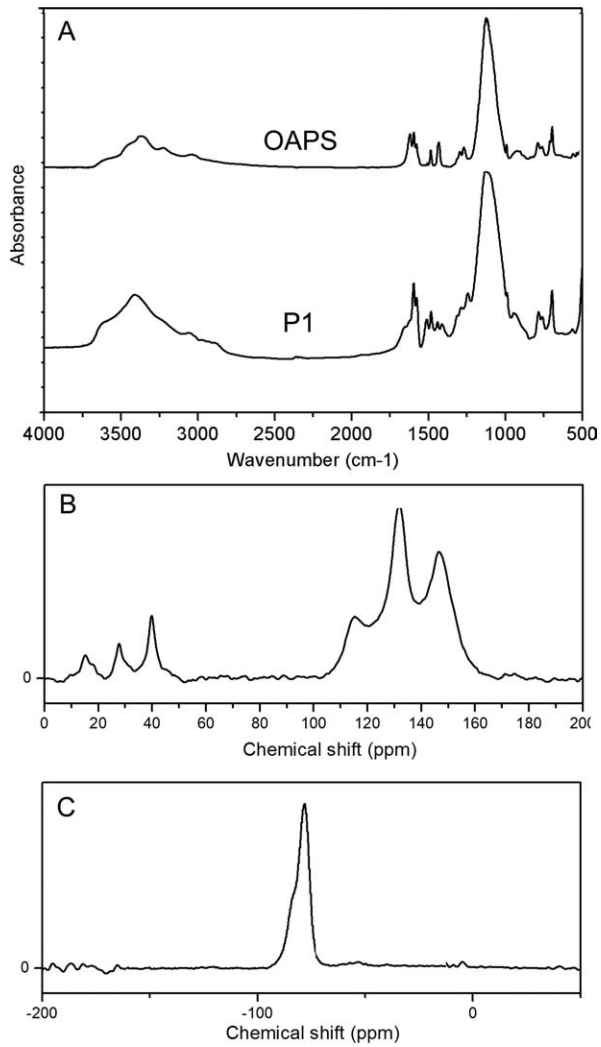

Figure 1 (A) IR, (B) solid-state ^{13}C-NMR, and (C) solid-state ^{29}Si-NMR spectra of OAPS and P1.

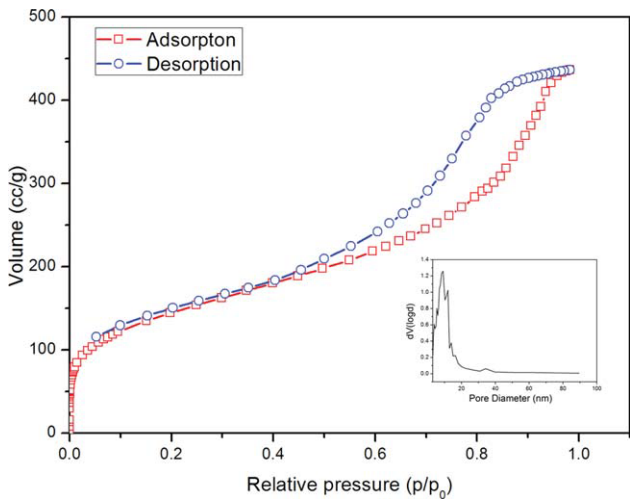

Figure 2 Nitrogen-sorption isotherm and corresponding pore-size-distribution curve of P1. [Color figure can be viewed in the online issue, which is available at wileyonlinelibrary.com.]

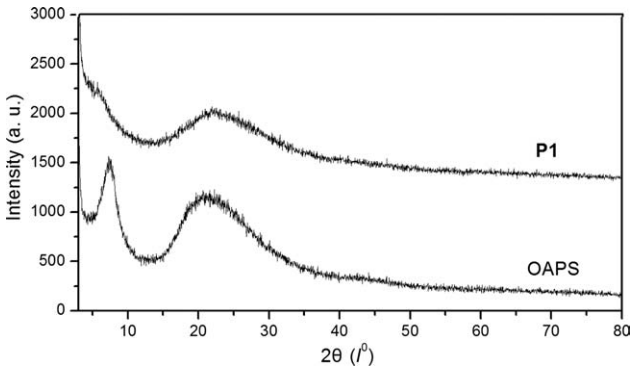

Figure 3 Powder XRD patterns of OAPS and P1.

aromatic carbons of the benzene rings and the carbon atoms of the alkyl groups [Fig. 1(B)]. The ^{29}Si-NMR spectrum of P1 showed overlapping of the lines and showed one signal at $\delta = -76.7$ ppm, which fell in the typical range for a POSS cage structure [Fig. 1(C)].[21,25] This result indicates that the cage structure of POSS was retained during the synthesis.

In summary, the combined results of FTIR, ^{13}C-NMR, and ^{29}Si-NMR spectroscopy clearly show that the POSS building blocks were successfully woven into the porous structure of the hybrid materials without obvious alteration of the structural characteristics of POSS.

Porous properties of the hybrid material

The hybrid material was subjected to BET measurements to evaluate the porosity of the polymers. Shown in Figure 2 are the BET curves of the hybrid material P1. According to the original IUPAC classification, the N_2 adsorption isotherm is not the classical type IV normally associated with mesoporous materials. Characteristic features of the type IV isotherm are its hysteresis loop, which is associated

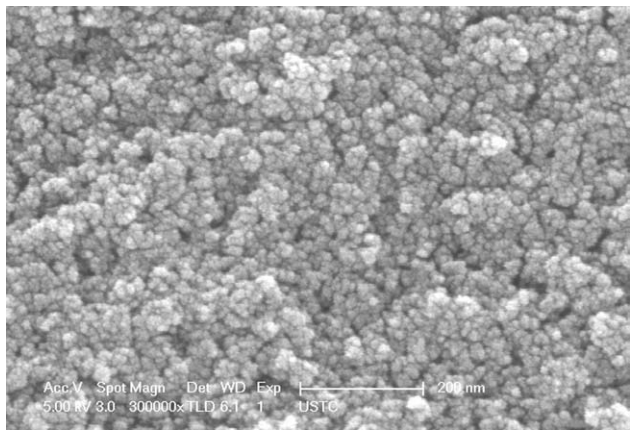

Figure 4 FESEM image of P1.

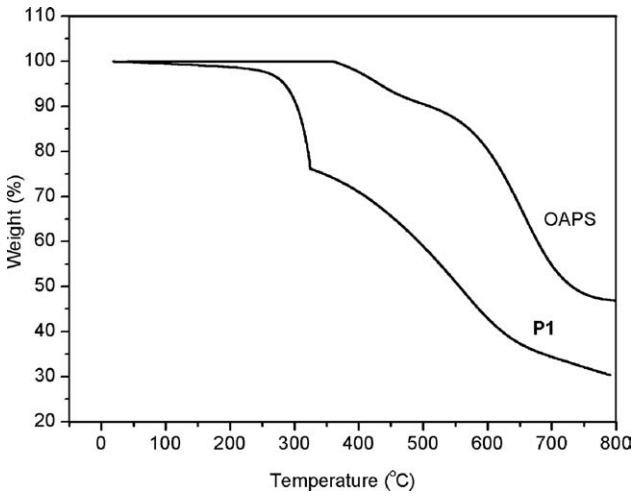

Figure 5 TGA thermograms of P1 and OAPS.

with capillary condensation taking place in mesopores, and the limiting uptake over a range of high p/p_0. Type IV isotherms are given by many mesoporous industrial adsorbents. The desorption isotherm does not close. This may suggest that the pores obtained are narrow and N_2 molecules are trapped in the pores.[26] According to BET calculation, the hybrid material had a specific surface area of 500.931 m^2/g, a pore volume of 0.563 cm^3/g, and an average pore size of 3.84 nm.

The porous structure of material was further investigated with Powder XRD and FESEM techniques. Figure 3 shows the Powder XRD studies of the materials OAPS and P1. OAPS showed a peak at 8° 2θ, which corresponded to a *d*-spacing of 1 nm. This diffraction peak could be explained by some long-range order in solid OAPS.[22,23] The broad halo at about 20° 2θ may have been associated with Si—O—Si linkages.[22,23] P1 exhibited broad diffraction peaks around 20° 2θ; this is typically observed for amorphous silica nanocomposites. P1 created a very rigid network with a very high viscosity that could not be expected to develop long-range order, so P1 did not show a diffraction peak at 8° 2θ.

Figure 4 shows the FESEM image of P1. As shown in Figure 4, the nanostructure of the material was homogeneous in appearance, and the porous structure of the materials was made from a large number of sizes of 20–30 nm particles, which were composed of pearl chainlike arrays. In the string of pearls with a large number of holes between the stacked structure, the existence of holes could be estimated from the figure and were mainly 10 nm and below in size, with a few holes of about 20 nm. This observation was consistent with the nitrogen-sorption measurements, which confirmed that the material had a mesostructure.

TGA

The hybrid mesoporous material was subjected to TGA to evaluate the thermal stability of the polymers. Figure 5 illustrates the TGA thermograms of P1 and OAPS. OAPS displayed an initial decomposition temperature of 400°C and a 5% mass loss temperature of about 460°C with a char yield of about 50 wt %. P1 showed excellent thermal stability. The initial decomposition temperature of P1 was about 250°C because the alkyl groups decomposed at this temperature. The decomposition of P1 occurring at about 325°C probably resulted from the fragmentation of the siloxane spacers. The char yield of P1 was about 30 wt %. All of these facts indicate that P1 showed excellent thermal stability.

CONCLUSIONS

In summary, in this article, we have reported a catalyst-free, one-pot method for preparing a novel covalently bonded POSS-containing organic–inorganic hybrid mesoporous nanocomposite at room temperature. The structures of the products were characterized by FTIR spectroscopy, NMR, N_2 adsorption isotherm, FESEM, and TGA. The material showed a specific surface area of 500.931 m^2/g, a pore volume of 0.563 cm^3/g, and an average pore size of 3.84 nm. The combined results of FTIR and solid-state ^{13}C-NMR and ^{29}Si-NMR spectroscopy clearly show that the POSS building blocks were successfully woven into the porous structure. The hybrid material showed excellent thermal stability.

References

1. Han, S. S.; Furukawa, H.; Yaghi, O. M.; Goddard, W. A. J Am Chem Soc 2008, 130, 11580.
2. Mckeown, N. B.; Budd, P. M. Chem Soc Rev 2006, 35, 675.
3. Wan, Y.; Wang, H.; Zhao, Q.; Klingstedt, M.; Terasaki, O.; Zhao, D. J Am Chem Soc 2009, 131, 4541.
4. Schmidt, J.; Weber, J.; Epping, J. D.; Antonietti, M.; Thomas, A. Adv Mater 2009, 21, 702.
5. Soler-Illia, G.; Sanchez, C.; Lebeau, B.; Patarin, J. Chem Rev 2002, 102, 4093.
6. Yang, Z.; Lu, Y.; Yang, Z. Chem Commun 2009, 2270.
7. Mizoshita, N.; Goto, Y.; Kapoor, M. P.; Shimada, T.; Tani, T.; Inagaki, S. Chem—Eur J 2009, 15, 219.
8. Hoffmann, F.; Cornelius, M.; Morell, J.; Fröba, M. Angew Chem Int Ed 2006, 45, 3216.
9. Zhang, C.; Babonneau, F.; Bonhomme, C.; Laine, R. M.; Soles, C. L.; Hristov, H. A.; Yee, A. F. J Am Chem Soc 1998, 120, 8380.
10. Chen, Y.; Kang, E. T. Mater Lett 2004, 58, 3716.
11. Huang, J. M.; Kuo, S. W.; Huang, H. J.; Wang, Y. X.; Chen, Y. T. J Appl Polym Sci 2009, 111, 628.
12. Feng, Y.; Jia, Y.; Guang, S.; Xu, H. J Appl Polym Sci 2010, 115, 2212.
13. Su, X.; Xu, H.; Deng, Y.; Li, J.; Zhang, W.; Wang, P. Mater Lett 2008, 62, 3818.
14. Cordes, D. B.; Lickiss, P. D.; Rataboul, F. Chem Rev 2010, 110, 2081.

15. Harrison, P. G.; Kannengisser, R. Chem Commun 1996, 415.
16. Morrison, J. J.; Love, C. J.; Manson, B. W.; Shannon, I. J.; Morris, R. E. J Mater Chem 2002, 12, 3208.
17. Zhang, L.; Abbenhuis, H. C. L.; Yang, Q.; Wang, Y.; Magusin, P. C. M. M.; Mezari, B.; van Santen, R. A.; Li, C. Angew Chem Int Ed 2007, 46, 5003.
18. Zhang, L.; Yang, Q.; Yang, H.; Liu, J.; Xin, H.; Mezari, B.; Magusin, P. C. M. M.; Abbenhuis, H. C. L.; van Santen, R. A.; Li, C. J Mater Chem 2008, 18, 450.
19. Goto, R.; Shimojima, A.; Kuge, H.; Kuroda, K. Chem Commun 2008, 6152.
20. Hagiwara, Y.; Shimojima, A.; Kuroda, K. Chem Mater 2008, 20, 1147.
21. Tamaki, R.; Tanaka, Y.; Asuncion, M. Z.; Choi, J.; Laine, R. M. J Am Chem Soc 2001, 123, 12416.
22. Tamaki, R.; Choi, J.; Laine, R. M. Chem Mater 2003, 15, 793.
23. Choi, J.; Tamaki, R.; Kim, S. G.; Laine, R. M. Chem Mater 2003, 15, 3365.
24. Barrett, E. P.; Joyner, L. G.; Halenda, P. P. J Am Chem Soc 1951, 73, 373.
25. Brus, J.; Urbanová, M.; Strachota, A. Macromolecules 2008, 41, 372.
26. Han, J.; Zheng, S. Macromolecules 2008, 41, 4561.